A&A 518, L104 (2010)
DOI: 10.1051/0004-6361/201014678

Astronomy & Astrophysics
Special feature

Herschel: the first science highlights

Letter to the Editor

Herschel-SPIRE observations of the Polaris flare: Structure of the diffuse interstellar medium at the sub-parsec scale⋆,⋆⋆

M.-A. Miville-Deschênes[1,9], P. G. Martin[9], A. Abergel[1], J.-P. Bernard[5], F. Boulanger[1], G. Lagache[1], L. D. Anderson[2], P. André[4], H. Arab[1], J.-P. Baluteau[2], K. Blagrave[9], S. Bontemps[16], M. Cohen[6], M. Compiegne[9], P. Cox[7], E. Dartois[1], G. Davis[8], R. Emery[12], T. Fulton[14], C. Gry[2], E. Habart[1], M. Huang[8], C. Joblin[5], S. C. Jones[11], J. Kirk[3], T. Lim[12], S. Madden[4], G. Makiwa[11], A. Menshchikov[4], S. Molinari[10], H. Moseley[13], F. Motte[4], D. A. Naylor[11], K. Okumura[4], D. Pinheiro Gonçalves[9], E. Polehampton[11,12], J. A. Rodón[2], D. Russeil[2], P. Saraceno[10], N. Schneider[4], S. Sidher[12], L. Spencer[11], B. Swinyard[12], D. Ward-Thompson[3], G. J. White[12,15], and A. Zavagno[2]

(Affiliations are available in the online edition)

Received 31 March 2010 / Accepted 11 May 2010

ABSTRACT

We present a power spectrum analysis of the *Herschel*-SPIRE observations of the Polaris flare, a high Galactic latitude cirrus cloud midway between the diffuse and molecular phases. The SPIRE images of the Polaris flare reveal for the first time the structure of the diffuse interstellar medium down to 0.01 parsec over a 10 square degrees region. These exceptional observations highlight the highly filamentary and clumpy structure of the interstellar medium even in diffuse regions of the map. The power spectrum analysis shows that the structure of the interstellar medium is well described by a single power law with an exponent of -2.7 ± 0.1 at all scales from 30″ to 8°. That the power spectrum slope of the dust emission is constant down to the SPIRE angular resolution is an indication that the inertial range of turbulence extends down to the 0.01 pc scale. The power spectrum analysis also allows the identification of a Poissonian component at sub-arcminute scales in agreement with predictions of the cosmic infrared background level at SPIRE wavelengths. Finally, the comparison of the SPIRE and IRAS 100 μm data of the Polaris flare clearly assesses the capability of SPIRE in maping diffuse emission over large areas.

Key words. ISM: clouds – ISM: structure – submillimetre: ISM – dust, extinction – turbulence

1. Introduction

Understanding the physical mechanisms involved in the formation of stars is still one of the major aspirations of modern astrophysics. One of the many aspects of this problem is related to the organisation of matter in the diffuse interstellar medium (ISM) as its structure provides the initial conditions for the formation of molecular clouds. The physics that impacts on the structure of the ISM is complex: it involves compressible and magnetic turbulent motions in a thermally unstable flow. Even though turbulence organises the flow up to scales of tens of parsec (Elmegreen & Scalo 2004), important non-linear physical processes take place at the sub-parsec scales. Being able to study the kinematics of the gas at such scale is essential but the density structure is also a key tracer of the physics involved.

Dust emission from uniformely heated regions of the local interstellar medium (i.e. exempt of local production of UV photons by stars) allows us to directly trace the density structure of the ISM. With its unprecedent angular resolution, the ESA *Herschel* Space Observatory (Pilbratt et al. 2010) allows us for the first time to study the structure of the ISM at the 0.01 pc scale over several square degrees. We present a first analysis of the 250, 350 and 500 μm emission maps of the Polaris flare obtained with the SPIRE instrument (Griffin et al. 2010). These observations are part of the "Evolution of interstellar dust" (Abergel et al. 2010) and "Gould Belt Survey" (André et al. 2010) SPIRE key projects.

The Polaris flare is a high Galactic latitude cirrus cloud, located at a distance ≤150 pc (Falgarone et al. 1998). It has significant CO emission (Heithausen & Thaddeus 1990; Meyerdierks & Heithausen 1996; Falgarone et al. 1998) and colder dust grains than typical diffuse clouds (Lagache et al. 1998; Bernard et al. 1999). As the Polaris flare does not show any sign of star-formation activity (only pre-stellar cores are detected with SPIRE – André et al. 2010), it is the archetype of the initial phases of molecular cloud formation. We present a power spectrum analysis of the dust continuum emission from big grains using SPIRE observations. These data allow us to study homogeneously the structure of the diffuse ISM from 0.01 to 8 pc.

2. SPIRE observations of the Polaris flare

The 250 μm SPIRE map, covering 10 square degrees of the brightest part of the Polaris flare, is shown in Fig. 1. The field was observed twice in nearly perpendical directions to optimize

⋆ *Herschel* is an ESA space observatory with science instruments provided by European-led Principal Investigator consortia and with important participation from NASA.

⋆⋆ Figures 4–6 are only available in electronic form at http://www.aanda.org

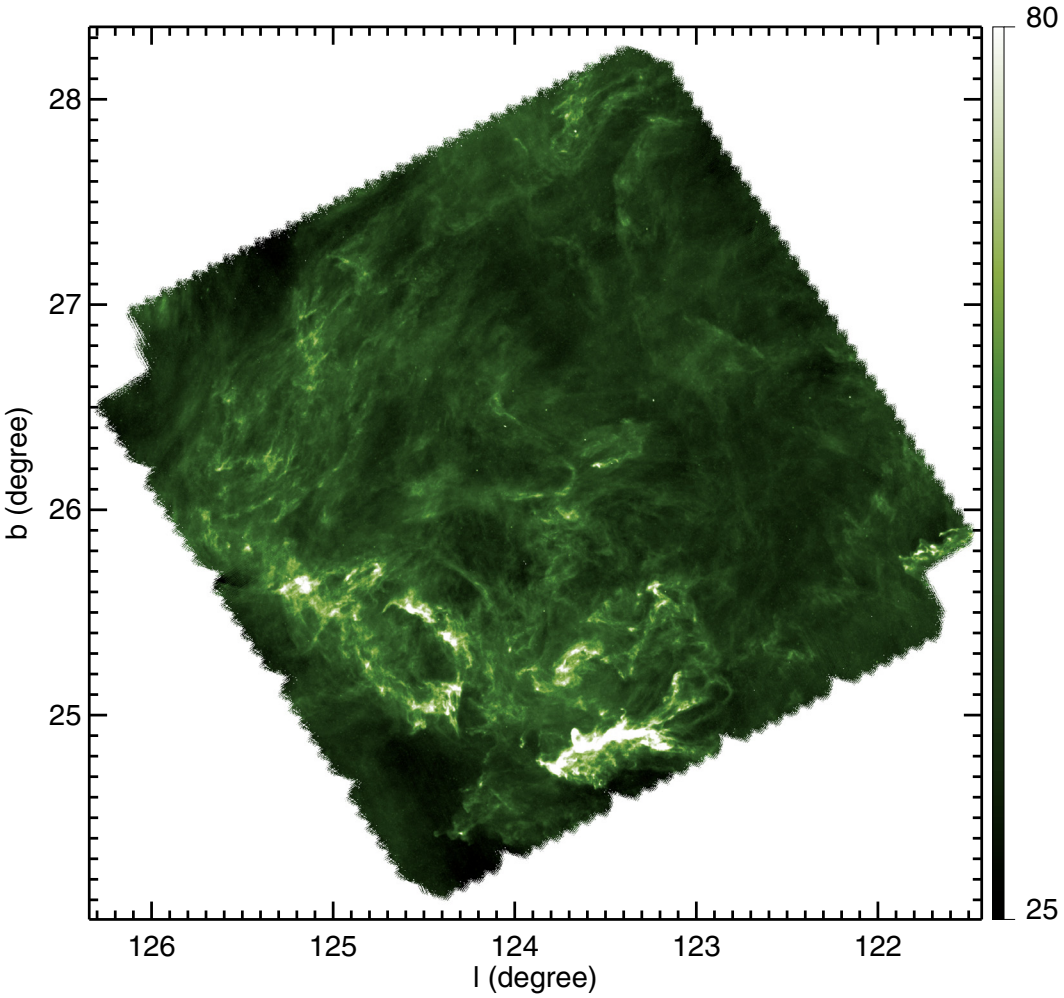

Fig. 1. SPIRE 250 μm map of the Polaris flare. Units are in MJy sr^{-1}. The zero level was set by correlation with the IRAS/IRIS 100 μm data.

the restoration of diffuse emission. The SPIRE data were processed with HIPE (version 2.0) applying standard corrections for instrumental effects and glitches. The $1/f$ noise component was removed using the "temperature drift correction" module, and naive maps were computed.

This map reveals for the first time the structure of the diffuse interstellar medium on scales ranging from 0.01 to 8 pc. Compared to the previous vision of the diffuse interstellar medium given by lower resolution observations (e.g. IRAS) these observations reveal a structure with strong contrast at small scales. Numerous small scale clumps are seen in the map even in the most diffuse regions (see examples in the Appendix). This high-resolution view of the diffuse ISM also reveals its highly filamentary structure with narrow threads of matter following the larger scale organisation. These observations bring new insights into the small scale structure of the ISM, and they will certainly help understand the physical processes dominating the dynamical evolution of matter towards the formation of stars. This task is obviously beyond the scope of the present paper.

3. Comparison with IRAS 100 μm: check of diffuse emission restoration and dust spectrum

The estimate of the power spectrum of the interstellar medium emission can only be done with observations that restore the power observed at all scales. This implies a great control of instrumental effects that could affect the baseline (additive effect) or the gain (multiplicative effect) of the detectors over the whole period of the observations. In order to assess the quality of the diffuse emission restoration by SPIRE over such a large field we made a comparison over the whole field with the 100 μm IRAS (IRIS) data (Miville-Deschênes & Lagache 2005) which are known to have a good description of the interstellar emission at all scales[1]. The main limitation of this exercise is the difference in wavelength between SPIRE and IRAS, but even though local variations of the dust emission spectrum are expected, the fact that both datasets are dominated by the emission from the big grain population is instructive.

We performed the following linear regression fit: $S(\lambda) = G \times S(100) + S_0$, where $S(100)$ is the 100 μm IRAS/IRIS map from which the average value of the cosmic infrared background at 100 μm (0.7 MJy/sr – Miville-Deschênes et al. 2007) was removed, and $S(\lambda)$ is the SPIRE map at wavelength λ, convolved to the IRAS resolution (4.3 arcmin) and projected onto the native 1.5′ grid of IRAS. The regression coefficients G and offsets S_0 found at each SPIRE wavelength are given in Table 1. Even though the correlations are good (correlation of 0.85), there is significant variation around the linear fit. Looking at

[1] In IRIS the variation with scale of the IRAS detectors gain was corrected and the emission at scales larger than 30′ was made consistent with DIRBE, which was designed for full control on systematic effects.

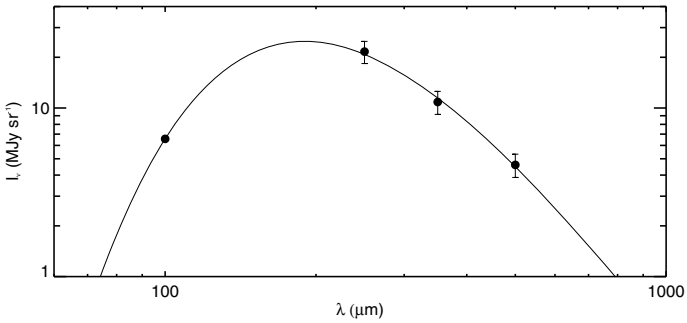

Fig. 2. Average big dust emission spectrum in the Polaris flare as determined by correlation of the SPIRE and 100 μm data over the whole field. In this plot the correlation coefficients (G in Table 1) were scaled to the average 100 μm brightness in the SPIRE field. The fit of the big grain emission spectrum gives $T_{\rm d} = 14.5 \pm 1.6$ and $\beta = 2.3 \pm 0.6$.

the difference map (i.e. $S(\lambda) - G \times S(100)$) localized variations are seen, which reflect expected modifications of the dust emission spectrum. These small and intermediate scale variations sit on a fainter large scale structure uncorrelated with the emission and therefore probably unrelated to variations of dust properties. This residual, which is less than 10% of the large scale emission fluctuations, could be attributed to residual imperfections in the data processing.

The factors G obtained for the SPIRE-IRAS correlation can be used to estimate the average dust emission spectrum in the field. The fit of a grey body[2] to the IRAS-SPIRE correlation coefficient shown in Fig. 2 gives $T_{\rm d} = 14.5 \pm 1.6$ and $\beta = 2.3 \pm 0.6$, in agreement with what was measured by Bernard et al. (1999) using PRONAOS and ISOPHOT data on a $30' \times 6'$ region in the brightest part of the Polaris flare ($T_{\rm d} = 13.0 \pm 0.8$ and $\beta = 2.2 \pm 0.3$). This provides a first order sanity check of the quality of the SPIRE gain calibration. In addition, looking at $(S(\lambda) - S_0)/S(100)$, we find no systematic correlation of G with intensity which agrees with the fact that the SPIRE diffuse emission calibration is not scale-dependent at scales larger than the IRAS beam.

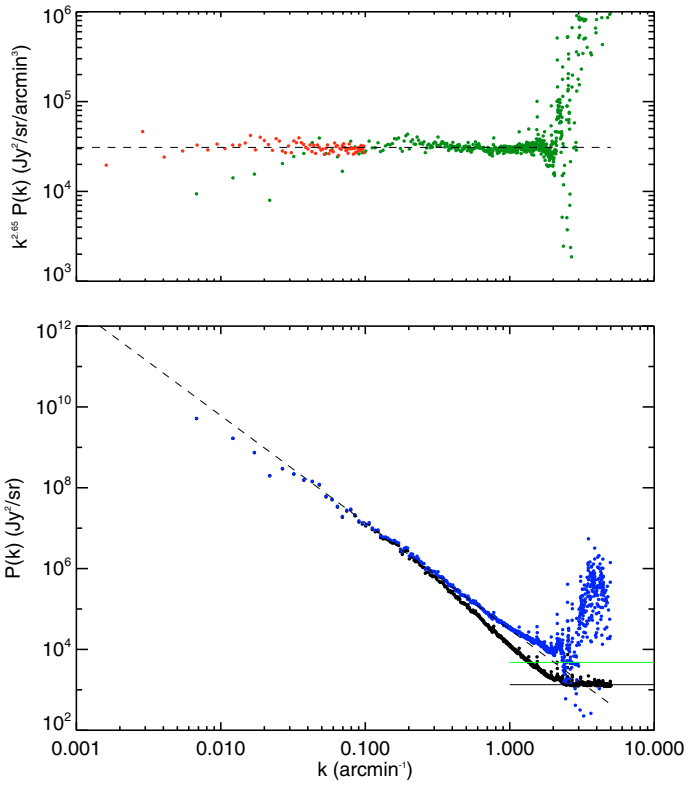

Fig. 3. Power spectrum of the SPIRE 250 μm map of the Polaris flare. *Bottom*: the black dots are the raw power spectrum (computed with an apodization of 0.97). The horizontal black line is the white noise level estimate. Blue dots are the power spectrum noise removed and divided by the psf estimated on Neptune observations. The green horizontal line and the dashed line are the source and interstellar components estimated from the blue dots power spectrum respectively, on scales $0.025 < k < 2$ arcmin^{-1}. *Top*: the green dots are the power spectrum of the interstellar component (i.e. corrected for noise, psf and sources) multiplied by $k^{2.65}$. The red dots are the power spectrum of the IRAS/IRIS 100 μm emission in a $12^\circ \times 12^\circ$ region centered on the SPIRE field. The dashed line is the same as in the bottom figure.

4. Power spectrum analysis

The power spectrum of the 250 μm map of the Polaris flare, converted to Jy^2/sr is shown in Fig. 3. The black dots in the bottom plot show the power spectrum computed on a $2.8^\circ \times 3.1^\circ$ area of the map where all data points are defined and from which bright point sources were removed. An apodization factor of 0.97 was applied prior to the Fourier Transform (Miville-Deschênes et al. 2002).

The power spectrum is typical of infrared emission of high Galactic latitude fields with a power-law type spectrum convolved by the instrument transfer function (ϕ), and a flat noise part (N) at high k. The power spectrum is modeled accordingly : $P(k) = \phi(k) P_{\rm sky}(k) + N(k)$. The white noise term stands out very clearly in all power spectra. Its level is estimated as the average of $P(k)$ for $0.75 k_{\rm max} < k < k_{\rm max}$, where $k_{\rm max}$ is the maximum k available (i.e. twice the pixel size – see Table 1). At each SPIRE wavelength this corresponds to scales smaller than the beam size where the noise dominates. The recovered noise levels are given in Table 1. They are comparable with the expected sensitivity for two repeats.

[2] $I_\nu \propto B_\nu(T_{\rm d}) \nu^{-\beta}$, where $T_{\rm d}$ and β are the big grain temperature and emissivity index, and B_ν is the Planck function.

The dark blue dots in Fig. 3 show the power spectrum of the 250 μm map, noise removed and divided by the transfer function $\phi(k)$ estimated using the official SPIRE beam profiles obtained on observations of Neptune. We emphasize here that the SPIRE beam shapes cannot be approximated by a Gaussian for the level of precision needed in this power spectrum analysis. Not taking into account the secondary lobes of the transfer function with a Gaussian would produce an artificial break in the power spectrum at scales of 0.1–0.2 arcmin^{-1} with a steepening of the slope at small scales.

Once corrected for noise and $\phi(k)$ the power spectrum shows a rather straight power law with a slight flattening at wavenumbers larger than 1 arcmin^{-1}, typical of a white component due to point sources and the unresolved cosmic infrared background (CIB) Poissonian fluctuations. To extract the interstellar contribution to the power spectrum we fitted the dark blue curve with $P_{\rm sky}(k) = A_{\rm ISM} k^\gamma + P_0$, where P_0 is the white level due to point sources and the CIB. The fit was done on scales between $k = 0.025$ arcmin^{-1}, to exclude the largest scales where the IRIS-SPIRE comparison showed significant differences, and about twice the *FWHM* (2.0, 1.2 and 0.86 arcmin^{-1} at 250, 350 and 500 μm respectively) to exclude scales contaminated by residual noise. The recovered γ and P_0 are given in Table 1. The

Table 1. SPIRE observations of the Polaris flare.

λ (μm)	Pixel size (arcsec)	*FWHM* (arcsec)	G	S_0 (MJy sr^{-1})	Noise (MJy sr^{-1})	γ	P_0 (Jy^2 sr^{-1})
250	6	18.1	3.3 ± 0.5 (0.01)	20.1 ± 3.1 (0.1)	1.26	−2.65 ± 0.10	$5 \pm 2 \times 10^3$
350	10	25.2	1.7 ± 0.3 (0.008)	10.1 ± 1.6 (0.05)	0.55	−2.69 ± 0.13	$4 \pm 2 \times 10^3$
500	14	36.9	0.7 ± 0.1 (0.003)	4.3 ± 0.7 (0.02)	0.34	−2.62 ± 0.17	$1 \pm 1 \times 10^3$

Notes. Columns 4 and 5: gain and offset coefficients of the SPIRE-IRIS 100 μm correlations. The uncertainty on G represents the rms of the ratio $S(\lambda)/S(100\,\mu\text{m})$ once the offset S_0 is removed from the SPIRE data. Similarly the uncertainty on S_0 is the rms of $S(\lambda) - G \times S(100\,\mu\text{m})$. These two uncertainties are correlated, but they give more realistic estimates compared to the statistical ones obtained with the linear regression fit (given in brackets). Column 6: noise level estimated directly on the power spectrum for $k > 0.75 k_{\max}$ ($3.75 < k < 5$ arcmin^{-1} at 250 μm). Column 7: power spectrum exponent of the interstellar component. Column 8: level of the Poissonian component associated with point sources and the CIB fluctuations. The fit of the power spectrum (γ and P_0) was done between $k = 0.025$ arcmin^{-1} and about twice the *FWHM* (2.0, 1.2 and 0.86 arcmin^{-1} at 250, 350 and 500 μm respectively).

uncertainties quoted in Table 1 include both the statistical error of the fit and a bias of a ±10% uncertainty on N. The increase of the uncertainty for γ from 250 to 500 μm is due to the range of scales on which the fit is done, which get shorter with increasing beam size. Even though the uncertainties for P_0 are significant, it is remarkable that the levels obtained agree very well with the predictions of Fernandez-Conde et al. (2008) for the CIB fluctuation level at the SPIRE wavelengths.

At 250 μm the slope of the power spectrum is $\gamma = -2.65 \pm 0.10$ at wavenumbers from $k = 0.025$ to 2.0 arcmin^{-1}. In the top panel of Fig. 3 the green dots represent the power spectrum (multiplied by $k^{2.65}$) of the SPIRE 250 μm map corrected for N, ϕ and P_0, leaving only the interstellar contribution. Within the uncertainties, the slopes are similar at all wavelengths (see Table 1). They are also compatible with the IRAS/IRIS 100 μm power spectrum measured on $12^\circ \times 12^\circ$ region centered on the SPIRE field[3] (red dots). However we note that the SPIRE power spectrum is systematically lower than IRAS for the first few large scale modes, in agreement with what was shown in Sect. 3. This effect, which could be partly due to suppresion of large scale modes in the SPIRE map-making, certainly deserves further investigation especially by comparing data in the common bands of SPIRE and Planck.

5. Discussion and conclusions

The power spectrum analysis of the 250, 350 and 500 μm SPIRE maps of the Polaris flare described here shows that the −2.7 slope measured at large scales using IRAS (Miville-Deschênes et al. 2007) or CO data (Stutzki et al. 1998) extends by more than one order of magnitude in scales, down to 30″. The high-resolution data obtained here on a 10 square degree field are in accordance with the results of Heithausen et al. (1998), who also found a slope of −2.7 on a similar range of scales combining high-resolution IRAM data of two 6′ by 8′ fields with lower resolution CfA and KOSMA data of a larger field. The analysis also reveals a Poissonian component at a level that agrees with CIB estimates.

As Polaris is uniformely heated by the interstellar radiation field, the dust grain temperature is likely to be rather uniform over the field. In these conditions brightness flutctuations in the SPIRE bands are dominated by dust column density fluctuations and the power spectrum of dust emission probes directly the power spectrum of the dust volume density in three dimensions. Assuming gas and dust are well mixed in this diffuse cloud, the power spectrum of the gas volume density would then have a slope of -2.7 ± 0.1 down to 0.01 pc. The constant slope of the power spectrum suggests that the turbulent cascade is still the main agent organizing the structure of the ISM at the 0.01 pc scale.

Finally it is important to point out that at this early phase of the *Herschel* mission it is impossible to rule out completely that the analysis is affected at some level by instrumental or processing effects. Nevertheless the comparison with IRAS/IRIS 100 μm and the use of the psf measured in-flight provide a coherent picture of the power spectrum analysis and show the capabilities of SPIRE at performing mapping of diffuse emission.

Acknowledgements. SPIRE has been developed by a consortium of institutes led by Cardiff University (UK) and including Univ. Lethbridge (Canada); NAOC (China); CEA, OAMP (France); IFSI, Univ. Padua (Italy); IAC (Spain); Stockholm Observatory (Sweden); Imperial College London, RAL, UCL-MSSL, UKATC, Univ. Sussex (UK); and Caltech/JPL, IPAC, Univ. Colorado (USA). This development has been supported by national funding agencies: CSA (Canada); NAOC (China); CEA, CNES, CNRS (France); ASI (Italy); MCINN (Spain); Stockholm Observatory (Sweden); STFC (UK); and NASA (USA).

References

Abergel, A., et al. 2010, A&A, 518, L96
André, Ph., et al. 2010, A&A, 518, L102
Bernard, J. P., et al. 1999, A&A, 347, 640
Elmegreen, B. G., & Scalo, J. 2004, ARAA, 42, 211
Falgarone, E., Panis, J. F., Heithausen, A., et al. 1998, A&A, 331, 669
Fernandez-Conde, N., Lagache, G., Puget, J. L., & Dole, H. 2008, A&A, 481, 885
Griffin, M. J., et al. 2010, A&A, 518, L3
Heithausen, A., & Thaddeus, P. 1990, ApJ, 353, L49
Heithausen, A., Bensch, F., Stutzki, J., Falgarone, E., & Panis, J. F. 1998, A&A, 331, L65
Lagache, G., Abergel, A., Boulanger, F., & Puget, J. L. 1998, A&A, 333, 709
Meyerdierks, H., & Heithausen, A. 1996, A&A, 313, 929
Miville-Deschênes, M. A., & Lagache, G. 2005, ApJS, 157, 302
Miville-Deschênes, M. A., Lagache, G., & Puget, J. L. 2002, A&A, 393, 749
Miville-Deschênes, M. A., Lagache, G., Boulanger, F., & Puget, J. L. 2007, A&A, 469, 595
Pilbratt, G. L., et al. 2010, A&A, 518, L1
Stutzki, J., Bensch, F., Heithausen, A., Ossenkopf, V., & Zielinsky, M. 1998, A&A, 336, 697

[3] The IRAS/IRIS power spectrum shown here has been corrected for noise, the transfer function and the CIB fluctuation level. It was scaled to match the SPIRE power spectrum at 10–15 arcmin scales.

[1] Institut d'Astrophysique Spatiale, CNRS/Université Paris-Sud 11, 91405 Orsay, France
[2] Laboratoire d'Astrophysique de Marseille (UMR 6110 CNRS & Université de Provence), 38 rue F. Joliot-Curie, 13388 Marseille Cedex 13, France
[3] Department of Physics and Astronomy, Cardiff University, Cardiff, UK
[4] CEA, Saclay, France
[5] Université de Toulouse; UPS; CESR; CNRS; UMR5187; 9 avenue du colonel Roche, 31028 Toulouse Cedex 4, France
[6] Radio Astronomy Laboratory, University of California, Berkeley, USA
[7] IRAM, Grenoble, France
[8] NOAC, PR China
[9] Canadian Institute for Theoretical Astrophysics, University of Toronto, ON M5S 3H8, Canada
[10] CNR - Istituto di Fisica dello Spazio Interplanetario, Roma, Italy
[11] Institute for Space Imaging Science, University of Lethbridge, Lethbridge, Canada
[12] Space Science Department, Rutherford Appleton Laboratory, Chilton, UK
[13] NASA - Goddard SFC, USA
[14] Blue Sky Spectrosocpy Inc, Lethbridge, Canada
[15] Department of Physics & Astronomy, The Open University, Milton Keynes MK7 6AA, UK
[16] CNRS/INSU, Laboratoire d'Astrophysique de Bordeaux, UMR 5804, BP 89, 33271 Floirac Cedex, France

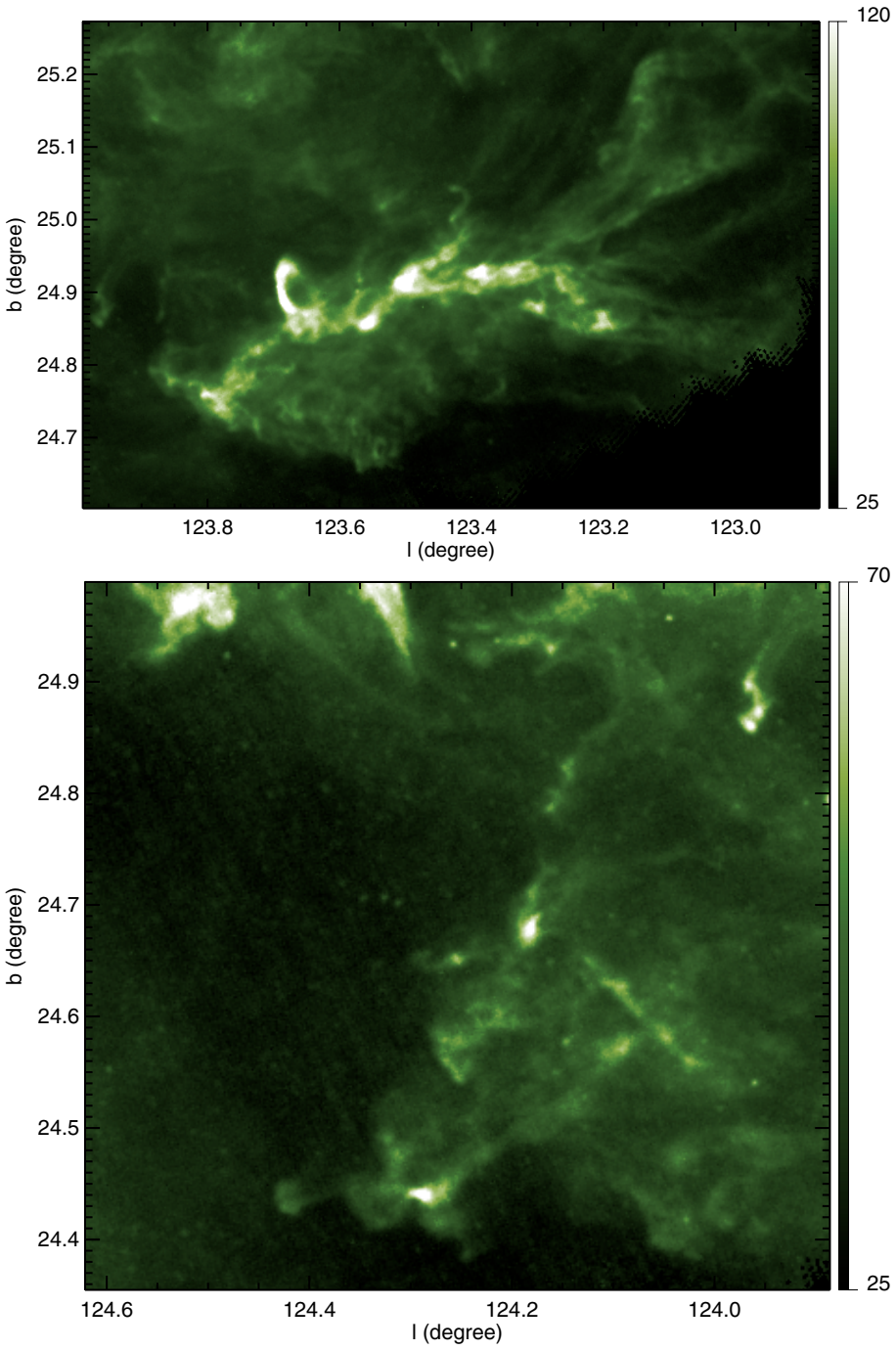

Fig. 4. Zoom on specific regions of the Polaris flare. Spire 250 μm data in MJy sr^{-1}.

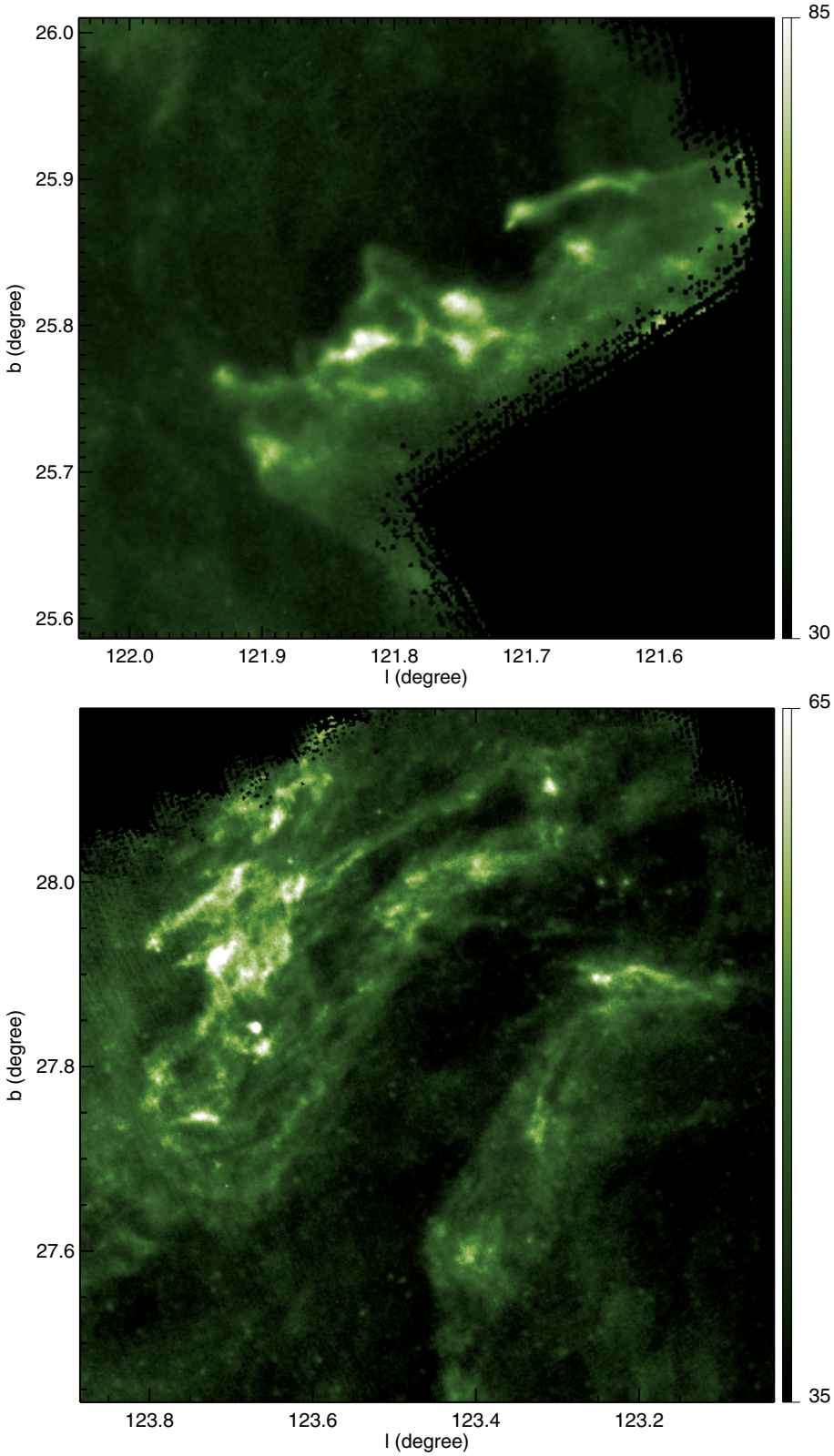

Fig. 5. Zoom on specific regions of the Polaris flare. Spire 250 μm data in MJy sr^{-1}.

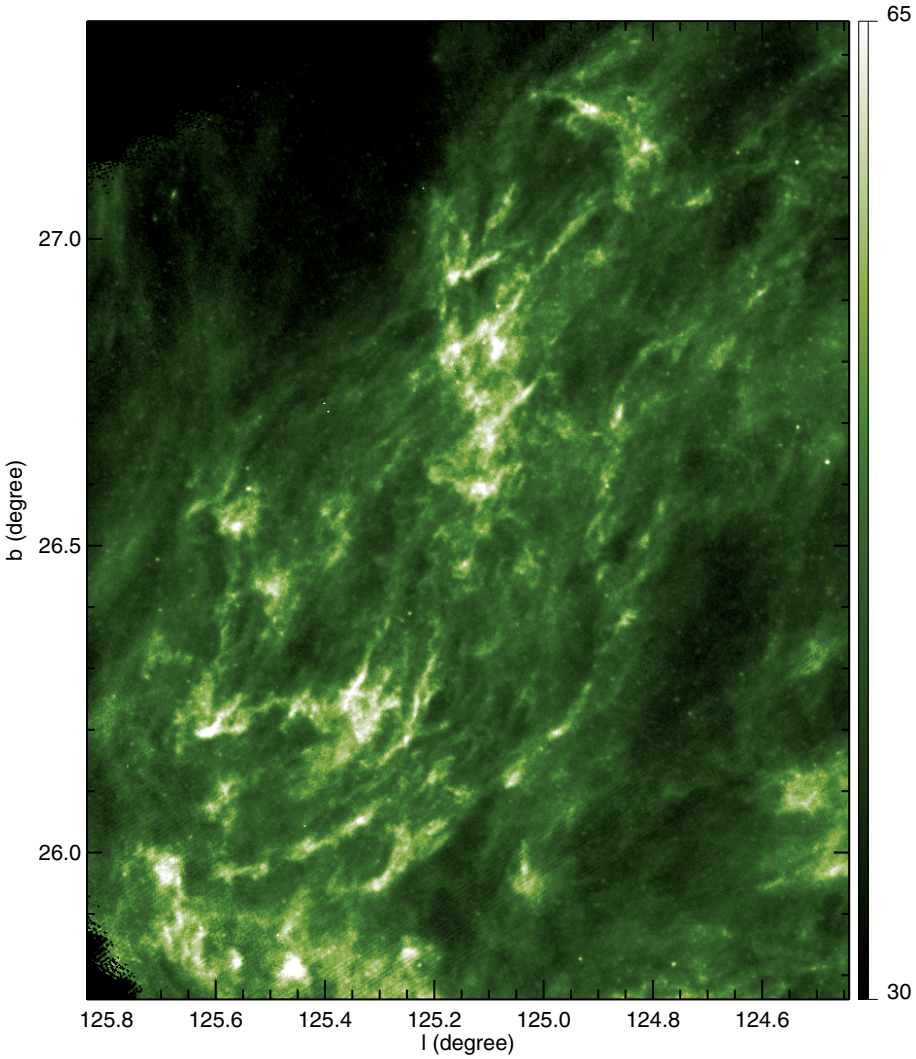

Fig. 6. Zoom on specific regions of the Polaris flare. Spire 250 μm data in MJy sr^{-1}.